Arabian Journal of Chemistry (2013) 6, 341–345

King Saud University

Arabian Journal of Chemistry

www.ksu.edu.sa
www.sciencedirect.com

ORIGINAL ARTICLE

Optical and electrical conducting properties of Polyaniline/Tin oxide nanocomposite

Manawwer Alam [a,*], Anees A. Ansari [b], Mohammed Rafi Shaik [c], Naser M. Alandis [c]

[a] *Research Center – College of Science, King Saud University, P.O. Box 2455, Riyadh, Saudi Arabia*
[b] *King Abdullah Institute for Nanotechnology, King Saud University, Post Box 2455, Riyadh, Saudi Arabia*
[c] *Department of Chemistry, King Saud University, Post Box 2455, Riyadh, Saudi Arabia*

Received 31 October 2011; accepted 23 April 2012
Available online 3 May 2012

KEYWORDS

Polyaniline;
SnO_2 nanoparticles;
Optical absorption spectra

Abstract Polyaniline(PANI)/Tin oxide (SnO_2) hybrid nanocomposite with a diameter 20–30 nm was prepared by co-precipitation process of SnO_2 through *in situ* chemical polymerization of aniline using ammonium persulphate as an oxidizing agent. The resulting nanocomposite material was characterized by different techniques, such as X-ray diffraction (XRD), Transmission Electron Microscopy (TEM), Fourier Transform Infrared spectroscopy (FT-IR) and Ultraviolet–Visible spectroscopy (UV–Vis), which offered the information about the chemical structure of polymer, whereas electron microscopy images provided information regarding the morphology of the nanocomposite materials and the distribution of the metal particles in the nanocomposite material. SEM observation showed that the prepared SnO_2 nanoparticles were uniformly dispersed and highly stabilized throughout the macromolecular chain that formed a uniform metal-polymer nanocomposite material. UV–Vis absorption spectra of PANI/SnO_2 nanocomposites were studied to explore the optical behavior after doping of nanoparticles into PANI matrix. The incorporation of SnO_2 nanoparticles gives rise to the red shift of π–π^* transition of polyaniline. Thermal stability of PANI and PANI/SnO_2 nanocomposite was investigated by thermogravimetric analysis (TGA). PANI/SnO_2 nanocomposite observed maximum conductivity (6.4×10^{-3} scm^{-1}) was found 9 wt% loading of PANI in SnO_2.

* Corresponding author. Tel.: +966 554738803.
E-mail address: malamiitd@gmail.com (M. Alam).

Peer review under responsibility of King Saud University.
http://dx.doi.org/10.1016/j.arabjc.2012.04.021

Production and hosting by Elsevier

1. Introduction

Conducting polymers have attracted much attention due to high electrical conductivity, ease of preparation, good environmental stability and wide variety of applications in light-emitting, biosensor chemical sensor, separation membrane and electronic devices (Stejskal, 2002; Thiyagarajan et al., 2003; Wu et al., 2007; Wang et al., 2008; Nesher et al., 2009; Yan et al., 2007; Yu et al., 2007; Ryu and Park, 2009). The most widely studied conducting polymers are polypyrrole, polyaniline, polythiophene etc. Additionally, PANI can coordinate

with metal ions, giving the multi-metallic system and also preparation of nanocomposite materials with other polymers (Luo et al., 2007; Deepa et al., 2007 Morrin et al., 2005; Yang et al., 2005).

Conducting polymers are characterized by a conjugated structure of alternating single and double bonds, the nature of their π-electron system, enhanced in oxidized or in reduced state and reversible redox activation in a suitable environment. The fundamental process of doping depends upon geometric parameters, such as bond length and bond angle. The charge is localized over the region of several repeating units. Conducting polymers have been found suitable for microelectronic device fabrication due to their excellent electric characteristics and ease of processability. Among these polymers PANI has emerged as promising candidate with great potential for practical uses such as light emitting diode, transparent electrode, electromagnetic radiation, corrosion protection of metals, gas sensors and humidity sensing and others (Wu et al., 2007a; Mentus et al., 2009; Li et al., 2008; Karslioglu et al., 2011). Polyanilines exist in a variety of protonation and oxidation forms. The most important form of polyaniline, green protonated emeraldine is produced by oxidation polymerization of aniline in aqueous acids. It is electrically conducting due to the presence of cation radicals in its structure. The positive charge on aniline units is balanced by negatively charged counter ions typically chloride anions (Li et al., 2008; Murugan et al.,2009).

Tin oxide is a widely used and studied n-type semiconductor, with a wide band gap (Eg = 3.6 eV) and crystalline structure. Several studies have been published on tin oxide based gas sensor, dye-sensitized solar cells, optical devices, optoelectronic devices, and hybrid microelectronic applications (Korosi et al., 2005; Konwer et al., 2010; Ningthoujan et al., 2007; Buron et al.,2011). The compound has lately also been examined as possible electrode material for lithium cells and photocatalysts. With properties such as transparency and semi conductivity it is an oxide of great interest from the technological point of view for gas sensor, humidity sensors white pigment for conducting coatings (Carreno et al., 2004; Ibarguen et al., 2007; Geng Li-na 2009; Zhang et al.,2006; Santos and Maruchin, 2006; Zhu et al., 2002; Du and Li, 2005; Dewyani et al., 2010). Tin oxide nanoparticles are synthesized through different chemical routes such as co-precipitation, hydrothermal sol–gel, sonochemical and polymer precursor method among others (Lina et al., 2007; Qin et al., 2008; Ansari et al., 2009).

In this paper, we report synthesis of tin oxide nanoparticles and PANI doped in SnO_2 nanoparticles using co-precipitation method and measured their optical, electrical and thermal properties of PANI/SnO_2 nanocomposite. The preparation of PANI/SnO_2 nanocomposite was characterized by XRD, TEM, UV–Vis, FT-IR, TGA and conductivity measurement.

2. Experimental methods

2.1. Materials

Aniline (BDH chemical Ltd., Poole, England) was double distilled before polymerization under reduced pressure, Ammonia (Winlab Chemical, UK), Ammonium Persulphate (Merck, India), Stannic Chloride (BDH chemical Ltd., Poole, England), ethanol and NH_4OH were procured from Merck India Ltd., Mumbai, India. The deionized water obtained from Millipore water purification system (Milli Q 10 TS) was used for the synthesis.

2.2. Synthesis of PANI

PANI was synthesized chemically in emeraldine salt form using redox process of aniline in the presence of ammonium peroxy disulfate (APS) as an oxidant and HCl. First double distilled aniline (20 ml) in 250 ml of 1 N HCl solution at room temperature was stirred for ½ h and subsequently 1 M (molar) APS solution (125 ml) was added at the rate of 10 drops/min. After adding complete solution of APS the stirring was continued for 4 h and resulting thick green solution was kept overnight for complete reaction. The precipitate was washed using 1 N (normal) HCl and tetrahydrofuron to remove oligomer and dried at 50 °C for 24 h. The PANI salt was converted into emeraldine base after treating with ammonium hydroxide solution.

2.3. Synthesis of PANI/SnO_2 nanocomposite

PANI/SnO_2 nanocomposite was synthesized by co-precipitation method. 1.0 g $SnCl_2$ $4H_2O$ was dissolved in 50 ml distilled water, after which 5 mL ammonium solution (1.0 M) was mixed under vigorous stirring at ambient temperature. On addition of ammonia solution, light yellow color precipitate occurs. Excess ammonia solution is added until pH 10 of the solution is obtained and added PANI (5–10 wt%).

Precipitate thus obtained was centrifuged and washed several times with distilled water to remove any residual reactant (NH^{+4}, Cl^{-}) and to obtain neutral pH after which it was dried in oven at 80 °C.

2.4. Characterization

Powder XRD data were carried out on a Rigaku Mini-flex X-ray diffractrometer (Japan) with Cu Kα radiation (λ = 1.5418 nm) at 30 kV and 15 mA with a scanning rate of 0.05/s in 2θ in a 2θ range from 10 to 70. FE-TEM image was carried out JEM-2100F model of JEOL at 120 kV accelerating voltage in order to observe the size of SnO_2 nanoparticle in PANI matrix. FT-IR spectra of the nanocomposite were recorded on a Nicolet iS 10, Thermo Scientific IR spectrometer (USA) in KBr medium at room temperature in the region 4000–400 cm^{-1}. The UV–Vis absorption spectra of the samples in methanol solvent were recorded in the range of 200–800 nm with a Shimadzu UV-2550, UV–vis spectrophotometer (Japan). Pellets of the pure PANI and PANI–SnO_2 were made with a compression-molding machine with hydraulic pressure. High pressure was applied (1.5–2.0 ton) to the sample to get hard round pellet (diameter = 1.5 cm, breadth = 2 mm); these pellets were used to measure conductivity. The electrical conductivity of the pure PANI and PANI/SnO_2 nanocomposite was measured with four-probe technique at room temperature. The current–voltage (I–V) characteristics were studied with Keithly 2400 source meter (USA) at room temperature. Voltage was applied to measure current through the sample. Thermogravimetric analysis (TGA) was performed with TGA/DSC1, Mettler Toledo AG, Analytical CH-8603, Schwerzenbach, Switzerland.

3. Result and discussion

Fig. 1 shows the results of powder XRD pattern of PANI/SnO_2 nanocomposite material synthesized through co-precipitation process after annealing at 200 °C. The results of XRD pattern indicate that nanocomposite is well crystalline and reveals all diffraction peaks, which are perfectly similar to the JCPDS data (Card No. 41–1445). The observed reflection planes resemble the tetragonal rutile SnO_2 nano-structure with values of lattice constants $a = 0.4742$ nm and $c = 0.3182$ nm. It can be seen that the reflection are markedly broadened, indicating a crystalline size of SnO_2 nano particle of 20–30 nm (Ansari et al.,2009).

FT-IR spectra (Fig. 2) of PANI and PANI/SnO_2 nanocomposite were measured to investigate the interaction between metal oxide and PANI. FT-IR spectrum of PANI shows all important absorption peaks 1575, 1519, 1325, 1291, 1138 and 834 cm^{-1}. The peaks at 1575 and 1519 cm^{-1} are assigned to C–C ring asymmetric and symmetric stretching vibrations. The peaks at 1325 and 1291 cm^{-1} correspond to N–H and C–C bending vibrations, respectively. The bands at 1138 and 834 cm^{-1} can be attributed to the in-plane and out-of-plane C–H bending, respectively. The corresponding peaks PANI/SnO_2 appear at 1597, 1560, 1321, 1294, 1116 and 827 cm^{-1}. The spectrum of the PANI/SnO_2 exhibits new peaks at 1400, 1625, 3259, 667, 559 and 437 cm^{-1}. The peak at 3259 cm^{-1} could be attributed to N–H stretching and at 1625 cm^{-1} to N–H bending vibration. The peaks at 667, 559 and 437 cm^{-1} correspond to Sn–OH, Sn–O–Sn bond and free oxi hydroxide. The band characteristic of SnO–N appears at 625 cm^{-1}.

UV–Vis spectroscopy was employed to characterize the optical properties of the synthesized nanocomposite materials. Fig. 3 shows the results of optical absorption spectra of SnO_2, PANI and PANI/SnO_2 nanocomposite materials in visible region. It can be seen that SnO_2 nanoparticles showed strong absorption in the UV light region (Fig. 3a). The spectrum show almost the same onset of absorption around 300 nm and the estimated band gap was 4.1 eV. Three characteristic absorption bands are observed in the spectrum of

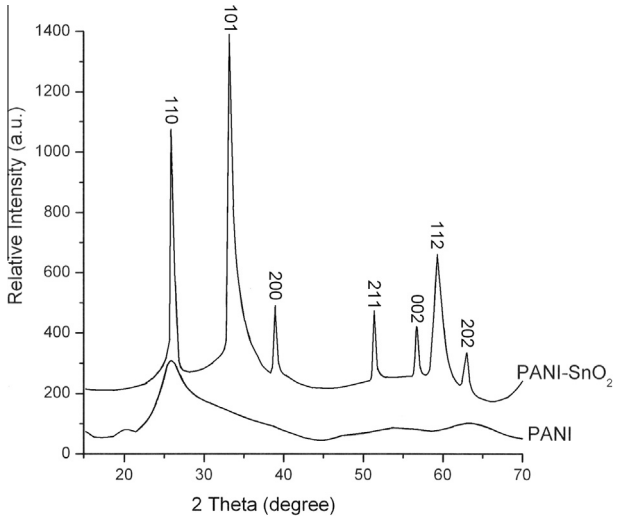

Figure 1 X-ray diffraction pattern of PANI and PANI/SnO_2 nanocomposite.

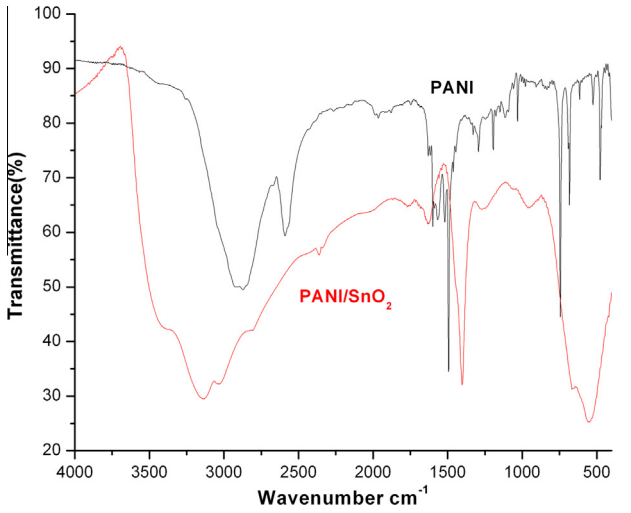

Figure 2 FT-IR spectra of PANI and PANI/SnO_2 nanocomposite.

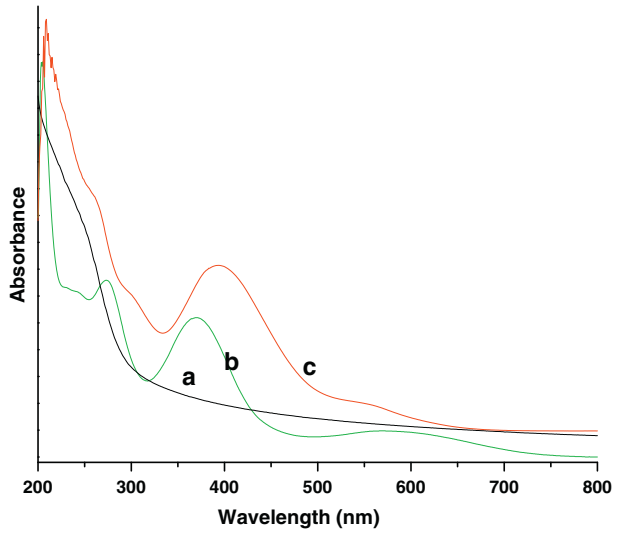

Figure 3 UV–Vis spectra of (a) SnO_2, (b) PANI and (c) PANI/SnO_2 nanocomposite.

PANI at 274, 370, 573 nm wavelength, which are attributed to π–π* conjugated ring systems, polaron-π* and π-polaron benzenoid to quinoid excitonic transition, respectively (Fig. 3b). This result indicated that PANI is completely transformed from the emeraldine salt to the emeraldine base form by the deprotonation of PANI with NH_4OH. The absorption band around 200–300 nm conjugated system and π-polaron band around 500–750 nm gradually disappeared in the nanocomposite spectrum and the band around 400 nm emerged. The absorption band at 400 nm is attributed to the excitation from the highest occupied molecular orbital of the benzenoid to the lowest unoccupied molecular orbital of the localized quinoid ring and the two surrounding imine nitrogens in the emeraldine base form of PANI (Fig. 3c). Furthermore, when tin oxide nanoparticles are dispersed in the PANI matrix, a significant change is measured in the absorption spec-

trum. The red shift of the absorption transition to higher wavelength may be due to the successful interaction of metal nanoparticles with the polymer chain. The characteristic features of absorption spectrum indicate that PANI/SnO_2 nanocomposite is in the conducting state.

FE-TEM micrograph was used to investigate the surface morphology of the synthesized PANI/SnO_2 nanocomposite material. The micrograph of PANI/SnO_2 nanocomposite shows a homogeneous, nanoporous structure that is uniformly distributed. FE-TEM observations give an overall view on a wide area allowing one to check that no large particles have been produced (Fig. 4).

Conductivity studies: The effect of PANI contents on the electrical conductivity of SnO_2 in PANI/SnO_2 nanocomposite. The nanocomposite with 5–10 wt% loading PANI in SnO_2 were prepared. The electrical conductivity of PANI(5 wt%)/SnO_2, PANI(6 wt%)/SnO_2, PANI(7 wt%)/SnO_2, PANI(8 wt%)/SnO_2, PANI(9 wt%)/SnO_2 and PANI(10 wt%)/SnO_2 were found to be 1.4×10^{-4} 1.9×10^{-4}, 5.4×10^{-4}, 1.7×10^{-3}, 5.4×10^{-3}, 6.4×10^{-3} and 8.4×10^{-4} scm^{-1}, respectively. The conductivity of these nanocomposite was found to be in the semiconducting range. After 9 wt% loading decreased the conductivity. This change due to the electrical charges was displaced inside the polymer (stronger localization).

Thermal Studies: The most significant and consistent study of heat stable polymer and nanocomposite is estimation of thermal stability. Thermal properties and interaction between polymer molecule and nanocomposite, can also be studied from the decomposition through TGA. TGA thermogram (Fig. 5) of PANI shows a sluggish decomposition curve spreading from 225 to 340 °C, although final decomposition was observed at 610 °C, at this temperature residue was about 10 wt%. Fifty percent weight loss was found at 305 °C, whereas 80% weight loss was observed at 340 °C. We have found that PANI/SnO_2 nanocomposite shows gentle decomposition with only 2% weight loss at 80 °C and 30% weight loss at 800 °C. These data show PANI/SnO_2 nanocomposite remarkable improvement in thermal stability.

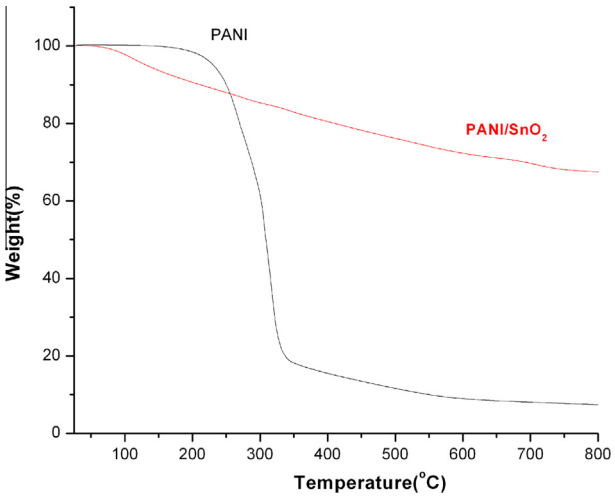

Figure 5 TGA thermogram of PANI/SnO_2 nanocomposite.

4. Conclusions

PANI/SnO_2 nanocomposite was successfully synthesized by *in situ* chemical polymerization of aniline using ammonium persulphate as an oxidizing agent. Formation of conducting emeraldine salt phases is confirmed by spectroscopic techniques. TEM images clearly showed that the polymer-encapsulated SnO_2 nanoparticles were uniformly distributed throughout the matrix and the particle diameter was relatively constant. UV/Vis, TGA and FT-IR studies confirm that there is strong chemical interaction between PANI and SnO_2 nanoparticles, which cause the red shift of UV and FT-IR characteristic bands. The absorption bands of PANI/SnO_2 nanocomposite are red shifted due to the quanta effect of SnO_2 and energy band match between PANI and SnO_2. PANI plays a key role in determining the transport mechanisms of nanocomposites. Maximum conductivity of PANI/SnO_2 nanocomposite prepared by the method used in this study was found to be 6.4×10^{-3} scm^{-1} at 9 wt% loading. We expect

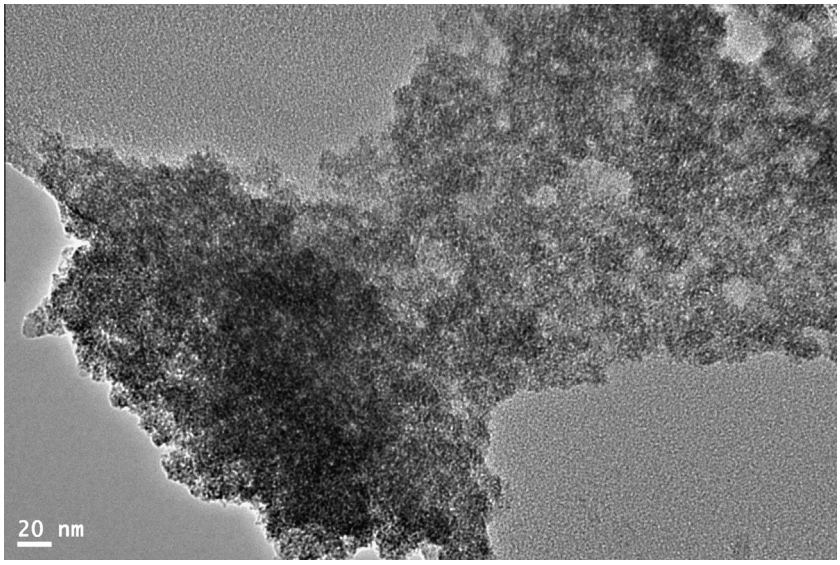

Figure 4 TEM micrograph of PANI/SnO_2 nanocomposite.

the PANI/SnO_2 nanocomposite microspheres have applications in new electric and photoelectric devices.

Acknowledgement

This project was supported by King Saud University, Deanship of Scientific Research, College of Science – Research Center.

References

Ansari, A.A., Solanki, P.R., Malhotra, B.D., 2009. Sens. Lett. 7, 64–71.
Carreno, N.L.V., Fajardo, H.V., Maciel, A.P., Volentini, A., Pontes, F.M., Probst, L.F.D., Leite, E.R., Longe, E., 2004. J. Mol. Catal. A: Chem. 207, 89–94.
Buron, C.C., Lakard, B., Monnin, A.F., Moutarlier, V., Lakard, S., 2011. Synth. Met. 161, 2162–2169.
Deepa, M., Ahmad, S., Sood, K.N., Alam, J., Ahmad, S., Srivastava, A.K., 2007. Electrochemi. Acta 52, 7453–7463.
Dewyani, P., Pardip, P., You-Kyong, S., Young, K.H., 2010. Sens. Actuators, B 148, 41–48.
Du, F., Li, Z.G., 2005. Mater. Lett. 59, 2563–2565.
Ibarguen, C.A., Mosquera, A., Parra, R., Castro, M.S., Paez, J.E.R., 2007. Mater. Chem. Phys. 101, 433–440.
Geng, Li.-na., 2009. Trans. Nonferrous Met. Soc. China 19, 678–683.
Korosi, L., Pupp, S., Meynen, V., Cool, P., Vansont, E.F., Dekany, I., 2005. Colloids Surf., A 268, 147–154.
Konwer, S., Pokhrel, B., Dolui, S.K., 2010. J. Appl. Polym. Sci. 116, 1138–1145.
Li, X.G., Li, A., Huang, M.R., 2008. Chem. Eur. J. 14, 10309–10317.
Lina, G., Yingqiang, Z., Xueliang, H., Shurong, W., Shoumin, Z., Shihua, W., 2007. Sens. Actuators, B 120, 568–572.
Luo, X., Killard, A.J., Smyth, M.R., 2007. Chem. Eur. J. 13, 2138–2143.
Mentus, S., Marjanovic, G.C., Trchova, M., Stejskel, J., 2009. Nanotechnology 20, 245601 (10pp).
Morrin, A., Ngamma, O., Killard, A., Moulton, S.E., Smyth, M.R., Wallace, G.G., 2005. Electroanalysis 17, 423–430.
Murugan, A.V., Muraliganth, T., Manthiram, A., 2009. Chem. Mater. 21, 5004–5006.
Nesher, G., Aylien, M., Sandaki, G., Avnir, D., Marom, G., 2009. Adv. Funct. Mater. 19, 1293–1298.
Ningthoujan, R.S., Sudarsan, V., Kulshereshta, S.K., 2007. J. Lumin. 127, 747–756.
Qin, L., Xu, J., Dong, X., Pan, Q., Cheng, Z., Xiung, Q., Li, F., 2008. Nanotechnology 19, 185705 (8pp).
Karslioglu, R., Uysal, M., Akbulut, H., 2011. J. Cryst. Growth 327, 22–26.
Ryu, J., Park, C.B., 2009. Angew. Chem., Int. Ed. 48, 4820–4823.
Santos, P.A., Maruchin, S., Menegoto, G.F., Zara, A.J., Pianaro, S.A., 2006. Mater. Lett. 60, 1554–1557.
Stejskal, J., 2002. Pure Appl. Chem. 74, 857–867.
Thiyagarajan, M., Kumar, J., Samuelson, L.A., Cholli, A.L., 2003. J. Macromol. Sci. A40, 1347–1355.
Wu, M., Zhang, L., Wang, D., Gao, J., Zhang, S., 2007. Nanotechnology 18, 385603 (7pp).
Wang, C.C., Song, J.F., Bao, H.M., Yang, C.Z., Shen, Q.D., 2008. Adv. Funct. Mater. 18, 1299–1306.
Wu, B.Q., Wang, Z., Xue, G., 2007a. Adv. Funct. Mater. 17, 1784–1789.
Yan, Y., Yu, Z., Hang, Y., Yuan, W., Wei, Z., 2007. Adv. Mater. 19, 3353–3357.
Yang, L., Yang, Z., Cao, W., 2005. Macromol. Rapid Commun. 26, 192–195.
Yu, Q., Zhu, J.J., Hu, X.Y., 2007. Chim. Acta 597, 151–156.
Zhang, D., Tao, L., Deng, Z., Zhang, J., Chen, L., 2006. Mater. Chem. Phys. 101, 275–280.
Zhu, J.J., Zhu, J.M., Lia, X.H., Fang, J.L., Zhou, M.G., Chen, H.Y., 2002. Material Lett. 53, 12–19.